PCCP

PAPER

View Article Online
View Journal | View Issue

Cite this: *Phys. Chem. Chem. Phys.*, 2016, **18**, 24549

Adsorption thermodynamics of two-domain antifreeze proteins: theory and Monte Carlo simulations

Claudio F. Narambuena,[a] Fabricio O. Sanchez Varretti[b] and Antonio J. Ramirez-Pastor*[a]

Received 10th June 2016,
Accepted 8th August 2016

DOI: 10.1039/c6cp03924c

www.rsc.org/pccp

In this paper we develop the statistical thermodynamics of two-domain antifreeze proteins adsorbed on ice. We use a coarse-grained model and a lattice network in order to represent the protein and ice, respectively. The theory is obtained by combining the exact analytical expression for the partition function of non-interacting linear k-mers adsorbed in one dimension, and its extension to higher dimensions. The total and partial adsorption isotherms, and the coverage and temperature dependence of the Helmholtz free energy and configurational entropy are given. The formalism reproduces the classical Langmuir equation, leads to the exact statistical thermodynamics of molecules adsorbed in one dimension, and provides a close approximation for two-dimensional systems. Comparisons with analytical data obtained using the modified Langmuir model (MLM) and Monte Carlo simulations in the grand canonical ensemble were performed in order to test the validity of the theoretical predictions. In the MC calculations, the different mechanisms proposed in the literature to describe the adsorption of two-domain antifreeze proteins on ice were analyzed. Indistinguishable results were obtained in all cases, which verifies the thermodynamic equivalence of these mechanisms and allows the choice of the most suitable mechanism for theoretical studies of equilibrium properties. Even though a good qualitative agreement is obtained between MLM and MC data, it is found that the new theoretical framework offers a more accurate description of the phenomenon of adsorption of two-domain antifreeze proteins.

1 Introduction

Antifreeze proteins (AFPs) help different organisms (insects, plants, fish) to survive at subzero temperatures.[1] This structurally diverse family of proteins links to the ice surface and inhibits the growth and re-crystallization of ice. The molecular binding mechanism depends entirely on a specific hydrogen bond match between the AFP and ice, with the contribution of van der Waals and hydrophobic forces.[2–4] These interactions evidently require intimate surface–surface complementarity between the receptor (AFP) and its ligand (ice).[5–7] The corresponding inhibition process has been considered as one of the many cases of crystal-growth inhibition by impurity adsorption.[8] In the past, there has been interest in the potential use of AFPs to protect cells and organs from freezing injury during cryopreservation.[9,10]

AFPs have diverse structural characteristics. For example, the protein denominated type III AFP is a peptide chain of 7 kDa (65 residues).[4] This protein has a compact fold with several β strands and one helical turn and a flat hydrophobic surface to bind to the ice crystal.[11,12] A protein called RD3 also exists, which is composed of two type III AFP domains connected by a flexible nine-residue linker.[13] The two domains are free to bind to the ice surface independently.[15] Then, each type III AFP can be modeled as one domain that adsorbs onto the ice surface, and the coarse-grained dimer model provides an accurate description of the RD3 protein. This representation has been widely used in the literature.[14–18]

In a recent paper, Can and Holland[16] studied the reversible adsorption of two different AFPs onto an ice crystal: a single-domain protein and a two-domain protein. A simple Langmuir isotherm was used for modeling the adsorption of the single-domain protein. In this framework, it is supposed that each adsorbed protein occupies one lattice site. In addition, a modified Langmuir model (MLM) was introduced in ref. 16 to account for the adsorption of the two-domain protein. The molecule was modeled as two identical units (or domains) connected in tandem

[a] *Departamento de Física, Instituto de Física Aplicada, Universidad Nacional de San Luis-CONICET, Ejército de Los Andes 950, D5700BWS San Luis, Argentina. E-mail: antorami@unsl.edu.ar*
[b] *Universidad Tecnológica Nacional, Facultad Regional San Rafael, Gral. Urquiza 314, 5600, San Rafael, Mendoza, Argentina*

by a flexible linker, and two possible adsorption states: with one of the domains adsorbed onto the ice surface allowing the second domain to freely diffuse only limited by the extent of the linker (state I), and with both domains adsorbed onto the ice surface (state II). The authors assumed that the adsorption occurs *via* a two-step mechanism. In the first step, the protein can be adsorbed from the bulk only in state I. In the second step, the protein can change its state from I to II. Under these considerations, the authors derived equations to describe the two adsorbed states of the protein.

An alternative approach, using the statistical mechanics formalism, was developed in previous work from our group.[17] In ref. 17, a lattice-gas model was applied to describe the adsorption of AFPs (with multiple adsorption states) onto an ice crystal. The proteins were modeled as chains of n identical units (domains) connected by flexible linkers, which can be adsorbed in n different adsorption states. A molecule adsorbed in the i-state is assumed to be a molecule occupying i sites on the lattice ($i = 1,\ldots,n$). From the point of view of the microscopic adsorption mechanism, the model supposes that the protein retains its structure after adsorption (transitions between different adsorption states are not allowed).

The theoretical scheme proposed in our previous article[17] provides the first exact model of molecules adsorbed in one dimension with n different adsorption states; includes as a particular case ($n = 2$) the phenomenology of the model derived by Can and Holland;[16] and leads to a close approximation for two-dimensional systems and multiple adsorbed states.

Even though many aspects of the problem have been studied in ref. 16 and 17, the theoretical description of the process of adsorption of AFPs on ice is a complex problem that does not have an exact statistical mechanical treatment in dimensions higher than one yet. Even more, there are no independent studies to support the reliability and validity of the theoretical results of ref. 16 and 17. One way of overcoming these theoretical complications is to use the Monte Carlo (MC) simulation method.[19–21] The MC technique is a valuable tool for studying surface molecular processes, which has been extensively used to simulate many surface phenomena.[22–24]

In this context, the main objectives of this work are: (1) to present analytical expressions for the main thermodynamic functions (adsorption isotherms, free energy and configurational entropy) characterizing the adsorption of two-domain AFPs on two-dimensional substrates; (2) to perform extensive MC simulations of the system under study, with special emphasis on the possible microscopic adsorption mechanisms; (3) to provide a comparative study that can be used to test the accuracy of the analytical results obtained here, and those reported in ref. 16; and (4) to corroborate the thermodynamic equivalence of the different adsorption mechanisms proposed in ref. 16 and 17.

The paper is organized as follows: the exact solution for the thermodynamic functions of two-domain proteins adsorbed in an infinite one-dimensional space is presented in Section 2. The functions are further extended to higher dimensions based on their exact form in one dimension and a connectivity ansatz. The basis of the MC simulation scheme is given in Section 3. Simulation results and theoretical predictions are discussed and compared in Section 4. Finally, the conclusions are drawn in Section 5.

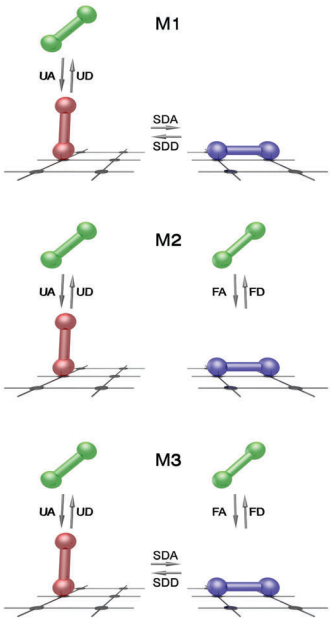

Fig. 1 Mechanisms M1, M2, and M3, for adsorption of antifreeze two-domain proteins. Nomenclature: UA, upright adsorption; FA, flat adsorption; UD, upright desorption; FD, flat desorption; SDA, second domain adsorption; and SDD, second domain desorption.

2 Theory: lattice-gas model and thermodynamic functions

The general statistical-mechanics derivation for a lattice-gas model of molecules with multiple adsorption states (LGMMAS) was presented in ref. 17. In this section, we will calculate the main thermodynamic functions for the specific application in our system.

Let us assume a lattice of M adsorption sites with lattice constant a, connectivity c and periodic boundary conditions. Under these conditions all lattice sites are equivalent, hence border effects will not enter our derivation.

N protein molecules are adsorbed on the surface with the following considerations: (1) each protein molecule is constituted by two identical units or domains, which are connected covalently by a peptide segment; (2) a molecule can adsorb on the lattice in two states or conformations (see Fig. 1). A molecule adsorbed in the 1-state (molecule adsorbed perpendicular to the surface or upright conformation) is assumed to be a molecule occupying 1 adsorption site on the lattice. On the other hand, a molecule adsorbed in the 2-state (molecule adsorbed parallel to the surface or flat conformation) is assumed to be a molecule occupying 2 nearest-neighboring adsorption sites on the lattice. Then, $N = N_1 + N_2$, N_i being the number of molecules adsorbed in the i-state.

Since the adsorbed proteins do not interact with each other (except the excluded volume interaction), all configurations with N_1 upright and N_2 flat molecules on M sites have the same energy:

$$E(N_1,N_2) = \varepsilon_1 N_1 + \varepsilon_2 N_2, \quad (1)$$

where ε_1 and ε_2 represent the adsorption energy for molecules adsorbed in upright and flat conformations, respectively. Therefore, the canonical partition function $Q_c(M,N_1,N_2,T)$ for this system can be written as:

$$Q_c(M,N_1,N_2,T) = \Omega_c(M,N_1,N_2)\exp\left[\frac{-E(N_1,N_2)}{k_B T}\right], \quad (2)$$

where $\Omega_c(M,N_1,N_2)$ is the number of ways to arrange N_1 upright molecules and N_2 flat molecules on a lattice of M sites and connectivity c; T is the absolute temperature and k_B is the Boltzmann constant. In order to simplify the calculus, the internal and vibrational contributions to the partition function are assumed to be a unitary factor in eqn (2).

For a one-dimensional lattice ($c = 2$), $\Omega_{c=2}(M,N_1,N_2)$ can be exactly calculated as the total number of permutations of the $N_1(N_2)$ indistinguishable protein molecules adsorbed in an upright(flat) configuration and N_0 empty sites, up the n_e entities, n_e being

$$n_e = N_1 + N_2 + N_0 = \sum_{i=1}^{2} N_i + M - \sum_{i=1}^{2} iN_i = M - \sum_{i=1}^{2}(i-1)N_i. \quad (3)$$

Accordingly,

$$\Omega_{c=2}(M,N_1,N_2) = \binom{n_e}{N} = \frac{\left[M - \sum_{i=1}^{2}(i-1)Ni\right]!}{N_1!N_2!\left[M - \sum_{i=1}^{2} iN_i\right]!}. \quad (4)$$

In general, $\Omega_c(M,N_1,N_2)$ can be calculated considering that the molecules are distributed completely at random on the lattice and assuming the arguments given by different authors,[25–27] to relate the configurational factor $\Omega_c(M,N_1,N_2)$ for any c, with the same quantity in one dimension ($c = 2$). Thus

$$\Omega_c(M,N_1,N_2) \approx [K(c,k)]^{N_2}\Omega_{c=2}(M,N_1,N_2) \quad (5)$$

where $K(c,k)$ is, in general, a function of the connectivity and the size of the adsorbed molecules. In the particular case of straight rigid k-mers (linear rigid particles containing k identical units, with each one occupying a lattice site) it follows that $K(c,k) = c/2$.

The Helmholtz free energy $F_c(M,N_1,N_2,T)$ is the thermodynamic potential that determines the spontaneity of the process in a canonical ensemble. This potential is related to $Q_c(M,N_1,N_2,T)$ through

$$\begin{aligned}\frac{F_c(M,N_1,N_2,T)}{k_B T} &= -\ln Q_c(M,N_1,N_2,T)\\ &= -\ln \Omega_c(M,N_1,N_2) + \frac{\varepsilon_1 N_1 + \varepsilon_2 N_2}{k_B T}.\end{aligned} \quad (6)$$

From eqn (4)–(6)

$$\begin{aligned}&\frac{F_c(M,N_1,N_2,T)}{k_B T}\\ &= -N_2\ln\left(\frac{c}{2}\right) - \ln(M-N_2)! + \ln(N_1)! + \ln(N_2)!\\ &+ \ln(M-N_1-2N_2)! + \frac{\varepsilon_1 N_1 + \varepsilon_2 N_2}{k_B T},\end{aligned} \quad (7)$$

which can be accurately written in terms of the Stirling approximation

$$\begin{aligned}\frac{F_c(M,N_1,N_2,T)}{k_B T} &= -N_2\ln\left(\frac{c}{2}\right) - (M-N_2)\ln(M-N_2)\\ &+ (M-N_2) + N_1\ln(N_1) - N_1 + N_2\ln(N_2)\\ &- N_2 + (M-N_1-2N_2)\ln(M-N_1-2N_2)\\ &- (M-N_1-2N_2) + \frac{\varepsilon_1 N_1 + \varepsilon_2 N_2}{k_B T}.\end{aligned} \quad (8)$$

The configurational entropy S_c, and the chemical potential corresponding to the molecule adsorbed in the i-state $\mu_{i,ads}$, can be calculated as[28]

$$S_c(M,N_1,N_2,T) = -\left(\frac{\partial F}{\partial T}\right)_{M,N_1,N_2}, \quad (9)$$

and

$$\mu_{1[2],ads} = \left(\frac{\partial F}{\partial N_{1[2]}}\right)_{T,M,N_{2[1]}}. \quad (10)$$

From eqn (8)–(10) it follows that

$$\begin{aligned}\frac{S_c(M,N_1,N_2,T)}{k_B} &= +N_2\ln\left(\frac{c}{2}\right) + (M-N_2)\ln(M-N_2)\\ &- (M-N_2) - N_1\ln(N_1) + N_1\\ &+ N_2\ln(N_2) + N_2\\ &- (M-N_1-2N_2)\ln(M-N_1-2N_2)\\ &+ (M-N_1-2N_2),\end{aligned} \quad (11)$$

$$\mu_{1,ads} = \ln(N_1) - \ln(M-N_1-2N_2) + \frac{\varepsilon_1}{k_B T}, \quad (12)$$

and

$$\begin{aligned}\mu_{2,ads} = &-\ln(M-N_2) + \ln(N_2) - 2\ln(M-N_1-2N_2)\\ &+ \frac{\varepsilon_2}{k_B T} - \ln\left(\frac{c}{2}\right).\end{aligned} \quad (13)$$

Then, by defining the lattice coverage $\theta_i = iN_i/M$, molar-free energy $f_c = F_c/M$ and molar configurational entropy $s_c = S_c/M$, eqn (8) and (11) can be rewritten in terms of the intensive variables θ_1, θ_2 and T,

$$\begin{aligned}\frac{f_c(\theta_1,\theta_2,T)}{k_B T} &= -\frac{\theta_2}{2}\ln\left(\frac{c}{2}\right) - \left(1-\frac{\theta_2}{2}\right)\ln\left(1-\frac{\theta_2}{2}\right)\\ &+ \theta_1\ln(\theta_1) + \frac{\theta_2}{2}\ln\left(\frac{\theta_2}{2}\right)\\ &+ (1-\theta_1-\theta_2)\ln(1-\theta_1-\theta_2)\\ &+ \frac{\varepsilon_1}{k_B T}\theta_1 + \frac{\varepsilon_2}{k_B T}\frac{\theta_2}{2},\end{aligned} \quad (14)$$

$$\frac{s_c(\theta_1,\theta_2,T)}{k_B} = +\frac{\theta_2}{2}\ln\left(\frac{c}{2}\right)+\left(1-\frac{\theta_2}{2}\right)\ln\left(1-\frac{\theta_2}{2}\right) - \theta_1\ln(\theta_1)-\frac{\theta_2}{2}\ln\left(\frac{\theta_2}{2}\right) - (1-\theta_1-\theta_2)\ln(1-\theta_1-\theta_2), \quad (15)$$

$$\frac{\mu_{1,ads}}{k_B T} = \ln(\theta_1)-\ln(1-\theta_1-\theta_2)+\frac{\varepsilon_1}{k_B T}, \quad (16)$$

and

$$\frac{\mu_{2,ads}}{k_B T} = \ln\left(1-\frac{\theta_2}{2}\right)+\ln\left(\frac{\theta_2}{2}\right)-2\ln(1-\theta_1-\theta_2)+\frac{\varepsilon_2}{k_B T}-\ln\left(\frac{c}{2}\right). \quad (17)$$

At equilibrium, the chemical potential of the adsorbed and solution phases are equal,

$$\frac{\mu_{i,ads}}{k_B T} = \frac{\mu_{sol}}{k_B T} = \frac{\mu^0_{sol}}{k_B T}+\ln C, \quad (18)$$

where μ_{sol} is the chemical potential of the protein in solution, μ^0_{sol} is the reference chemical potential and C is the protein concentration in the bulk solution.

Introducing eqn (18) in eqn (16) and (17), the partial adsorption isotherms can be obtained,

$$\theta_1 = \frac{K_1 C}{1+K_1 C}\sqrt{1-\frac{cK_2 C}{cK_2 C+\frac{1}{2}(1+K_1 C)^2}}, \quad (19)$$

$$\theta_2 = 1-\sqrt{1-\frac{cK_2 C}{cK_2 C+\frac{1}{2}(1+K_1 C)^2}}, \quad (20)$$

and

$$\theta = \theta_1+\theta_2, \quad (21)$$

where $K_i = \exp[\beta(\mu^0_{sol}-\varepsilon_i)]$ is the equilibrium binding constant between the protein in the solution and the molecule adsorbed in the i-state.

The explicit forms of eqn (19)–(21) could be of interest to study the kinetic properties of the system. In fact, the ice crystal growth rates as a function of protein concentration can be described using the model presented by Kubota and Mullin.[29] In ref. 29, the authors propose the following expression to characterize the crystal growth from aqueous solution in the presence of impurities,

$$V/V_0 = 1-\alpha\theta_{eq}, \quad (22)$$

where V is the step velocity in the presence of impurities, V_0 is the step velocity in a pure system, θ_{eq} is the fractional coverage by adsorbed impurities on the surface, and α is an effectiveness factor.

Eqn (22) connects equilibrium (θ_{eq}) and kinetic (V) quantities. In the original work,[29] the connection is carried out using the classical Langmuir isotherm. By replacing the Langmuir equation by eqn (19)–(21), the model by Kubota and Mullin could be applied to a system of two-domain AFPs adsorbed on ice. This issue is out of the scope of the present work, and will be the object of future research in our group.

3 General Monte Carlo scheme

In order to study the adsorption of two-domain antifreeze proteins on ice, a general MC scheme in the grand canonical ensemble was implemented. The ice crystal surface was represented by a square lattice of $M = L \times L$ adsorption sites, and the protein was modeled as a dimer molecule with two possible adsorption states. As it is shown in Fig. 1, (1) each domain of the protein can be adsorbed on only one site of the lattice, and (2) each lattice site can be in three possible states, namely empty or occupied with a domain belonging to an upright or a flat protein.

Then, given a square lattice of M equivalent adsorption sites in contact with a solution at temperature T and protein concentration C, the algorithm to carry out an elementary Monte Carlo Step (MCS) is the following:

1. A lattice site i is chosen at random.

2. If the site i is empty, then one of the two possible orientations of the protein is chosen: 1-state (upright configuration) with probability P_1, and 2-state (flat configuration) with probability $1-P_1$.

2.1. If the state selected in step 2 is 1, then an attempt is made to adsorb a protein in an upright orientation with probability

$$\min\left\{1, C\exp\left(-\frac{\Delta E}{k_B T}\right)\frac{P_2}{P_1}\right\}, \quad (23)$$

where ΔE is the difference between the energies of the final (New) and initial (Old) states (see Appendix).

2.2. If the state selected in step 2 is 2, a site j is randomly chosen among the nearest neighbors of the site i.

2.2.1. If the site j is empty, then an attempt is made to adsorb a protein in a flat orientation with probability

$$\min\left\{1, C\exp\left(-\frac{\Delta E}{k_B T}\right)\frac{1-P_3}{1-P_1}\right\}. \quad (24)$$

2.2.2. If the site j is occupied, then the attempt is rejected.

3. If the site i is occupied by a protein in the 1-state, then one of the two following processes is chosen: desorption (the protein returns to the bulk solution) with probability P_2, and change from the 1-state to the 2-state with probability $1-P_2$.

3.1. If the process selected in step 3 is desorption, then an attempt is made to desorb a protein from an upright orientation with probability

$$\min\left\{1, \frac{1}{C}\exp\left(-\frac{\Delta E}{k_B T}\right)\frac{P_1}{P_2}\right\}. \quad (25)$$

3.2. If the process selected in step 3 is change from the 1-state to the 2-state, a site j is randomly chosen among the nearest neighbors of the site i.

3.2.1. If the site j is empty, then an attempt is made to change the adsorption state of the protein from an upright to flat configuration with probability

$$\min\left\{1, \exp\left(-\frac{\Delta E}{k_B T}\right)\frac{P_3}{1-P_2}\right\}. \quad (26)$$

3.2.2. If the site j is occupied, then the attempt is rejected.

4. If the site i is occupied by a domain belonging to a protein adsorbed in the 2-state, then one of the two following processes is chosen: change from the 2-state to the 1-state with probability P_3, and desorption (the protein returns to the bulk solution) with probability $1 - P_3$.

4.1. If the process selected in step 4 is change from the 2-state to the 1-state, a site j is randomly chosen among the nearest neighbors of the site i.

4.1.1. If the sites i and j are occupied by two domains belonging to the same molecule, then an attempt is made to change the adsorption state of the protein from a flat to upright configuration with probability

$$\min\left\{1, \exp\left(-\frac{\Delta E}{k_B T}\right)\frac{1-P_2}{P_3}\right\}. \quad (27)$$

If the change is accepted, the domain on site i is detached from the surface.

4.1.2. Otherwise, the attempt is rejected.

4.2. If the process selected in step 4 is desorption, then an attempt is made to desorb a protein from a flat orientation with probability

$$\min\left\{1, \frac{1}{C}\exp\left(-\frac{\Delta E}{k_B T}\right)\frac{1-P_1}{1-P_3}\right\}. \quad (28)$$

5. Repeat from step 1 M times.

A detailed analysis of the calculation of the acceptance criteria in eqn (23)–(28) is provided in section Appendix.

According to the values chosen for the probabilities P_1, P_2 and P_3, different adsorption mechanisms can be considered. Following the previous literature,[16,17] three adsorption mechanisms were studied and compared in this work (see Fig. 1).

In the first mechanism (M1),[16] the two-domain proteins adsorb onto the ice lattice in a two-step process. In the initial stage, the molecules attach to the surface with an upright orientation (occupying one lattice site). Subsequently, the protein can change its state to 2-state (flat configuration), with both domains adsorbed onto the ice surface. The desorption process is also a two-step process. Namely, a protein in the 2-state can only change to the 1-state (returning to an upright configuration). Once in the 1-state, the protein can desorb from the ice surface.

In terms of the P_i values, the conditions corresponding to M1 are satisfied if $P_1 = 1$: a protein can only be adsorbed on the surface in the 1-state; $P_2 = 1/2$: a protein in the 1-state can either be desorbed from the surface, or change its state to the 2-state (both options are equally probable); and $P_3 = 1$: a protein in the 2-state can only change to the 1-state.

The second mechanism (M2)[17] supposes that the protein can be adsorbed in either an upright or flat orientation with equal probability ($P_1 = 1/2$). Transitions from the 1-state to the 2-state (and from the 2-state to the 1-state) are not allowed. Accordingly, an adsorbed protein can only be desorbed from the surface ($P_2 = 1$ and $P_3 = 0$).

The third mechanism (M3) is the combination of the two mechanisms described above. The protein can be adsorbed/desorbed with an upright and flat orientation, and can change its configuration from the 1(2)-state to the 2(1)-state. In this case, $P_1 = P_2 = P_3 = 1/2$.

Table 1 summarizes the values of P_1, P_2 and P_3 corresponding to the three adsorption mechanisms studied in this work.

In our MC simulations, the equilibrium state can be well reproduced after discarding the first $m' = 10^6$ MCS. Then, averages are taken over $m = 10^6$ MCS successive configurations. The initial configuration of the system is an empty square lattice, and the final configuration obtained for a given concentration is used as the initial configuration for the next (higher) concentration.

Thermodynamic quantities, such as the total and partial isotherms and adsorption energy per site $u = E/M$, are obtained as simple averages

$$\theta_1 = \frac{\langle N_1\rangle}{M}, \quad (29)$$

$$\theta_2 = \frac{2\langle N_2\rangle}{M}, \quad (30)$$

$$\theta = \theta_1 + \theta_2 = \frac{\langle N_1\rangle + 2\langle N_2\rangle}{M}, \quad (31)$$

and

$$u = \frac{\varepsilon_1\langle N_1\rangle + \varepsilon_2\langle N_2\rangle}{M}, \quad (32)$$

where the factor two in eqn (30) is due to the fact that each protein adsorbed in a flat orientation occupies two sites on the lattice; and $\langle\cdots\rangle$ means the average over the MC simulation runs.

The Helmholtz free energy per site $f = F/M$ is calculated by using the well-known thermodynamic integration method.[19] The method in the grand canonical ensemble relies on the integration of the chemical potential μ on coverage along a reversible path between an arbitrary reference state and the desired state of the system. This calculation also requires the knowledge of the Helmholtz free energy per site in the reference state f_0. Thus,

$$f = f_0 + \frac{\int_0^N \mu \mathrm{d}N'}{M}. \quad (33)$$

The determination of f_0 is trivial [$f_0 = F(M, N_1 = 0, N_2 = 0, T)/M = 0$]. Finally, the entropy per site s is calculated as the difference between the internal energy and energy free:[28]

$$\frac{s}{k_B} = \frac{u}{k_B T} - \frac{f}{k_B T}. \quad (34)$$

4 Results

It is instructive to begin by discussing the behavior of the system for the one-dimensional case, where the theoretical formalism presented in Section 2 provides a rigorous solution.

Table 1 Trial probability values corresponding to the three mechanisms studied in this work

Trial probability	Mechanism 1	Mechanism 2	Mechanism 3
P_1	1	$\frac{1}{2}$	$\frac{1}{2}$
P_2	$\frac{1}{2}$	1	$\frac{1}{2}$
P_3	1	0	$\frac{1}{2}$

In this way, the accuracy of the simulation data can be asserted by comparison with exact results.

Fig. 2(a) shows the total and partial adsorption isotherms for a one-dimensional lattice with $\varepsilon_1/k_BT = -2$ and $\varepsilon_2/k_BT = -4$. Symbols represent simulation data† and lines correspond to theoretical results from eqn (19)–(21) with $c = 2$. The figure also includes curves obtained from MLM[16] (dashed lines). In this framework, the partial and total adsorption isotherms take the form

$$\theta_1 = \frac{-1 - K_1C + \sqrt{(1+K_1C)^2 + 4K_1K_2C}}{2K_2}, \quad (35)$$

The adsorption process can be explained as follows. For low bulk protein concentrations, molecules are preferentially adsorbed in the 2-state (flat orientation). As the protein concentration increases, the amount of protein adsorbed in the 1-state (upright configuration) also increases, and a competition between flat and upright molecules is stated. This behavior is clearly reflected by the flat partial isotherm: at low C, θ_2 is an increasing function of the concentration, goes through a maximum around $\ln C \approx -2$ ($\theta_2 \approx 0.72$), and finally tends asymptotically to zero for higher values of C. In this limit, the lattice is basically filled with upright proteins.

$$\theta_2 = \frac{-1 - K_2 - 2K_1C - K_1^2C^2 - 3K_1K_2C + (1+K_2+K_1C)\sqrt{(1+K_1C)^2 + 4K_1K_2C}}{K_2 - K_1K_2C + K_2\sqrt{(1+K_1C)^2 + 4K_1K_2C}}, \quad (36)$$

and

$$\theta = \frac{1}{2K_1K_2C} + \frac{1}{2K_2} + 1 - \sqrt{\left(\frac{1}{2K_1K_2C} + \frac{1}{2K_2}\right)^2 + \frac{1}{K_1K_2C}}. \quad (37)$$

An excellent agreement is obtained between the exact and simulation data, validating the applicability the MC method introduced here. Qualitative similar results are obtained from MLM.

The simulation data in Fig. 2(a) were calculated using M3. However, indistinguishable results are obtained using M1 and M2. As an example, Fig. 2(b) shows the convergence towards the steady state of θ_1 and θ_2 for a typical case: $c = 2$, $\varepsilon_1/k_BT = -2$, $\varepsilon_2/k_BT = -4$ and $\ln C = -1$. Black, blue and red lines represent results obtained using M1, M2 and M3, respectively. These curves are obtained by average on 10 000 realizations of the simulations for each mechanism. The behavior of each mechanism is different in the early steps of the simulation, but M1, M2 and M3 converge to the same equilibrium value. These results cannot be directly connected to the real dynamics, but guarantee the thermodynamic equivalence of the different adsorption mechanisms proposed in Section 3. This finding has important theoretical implications, demonstrating that the kinetic equations derived in ref. 16 provide equilibrium states directly comparable to the predictions of statistical mechanics models.

Hereafter, we present the analysis of the adsorption of proteins on two-dimensional substrates. For this purpose, square lattices of $M = 120 \times 120$ sites and periodic boundary conditions were simulated. With this lattice size we verified that finite size effects are negligible. In order to build the adsorption isotherm, the protein concentration was varied between $\ln C = -15$ and $\ln C = 15$. In addition, as in the one-dimensional case, it was proved that M1, M2 and M3 lead to identical equilibrium states.

Fig. 3 shows the total and partial adsorption isotherms for a square lattice with $\varepsilon_1/k_BT = -2$ and $\varepsilon_2/k_BT = -4$. Thus, each domain has the same adsorption energy $-2k_BT$. Symbols are as in Fig. 2.

† The simulations have been performed for one-dimensional lattices of $M = 1200$ sites and periodic boundary conditions.

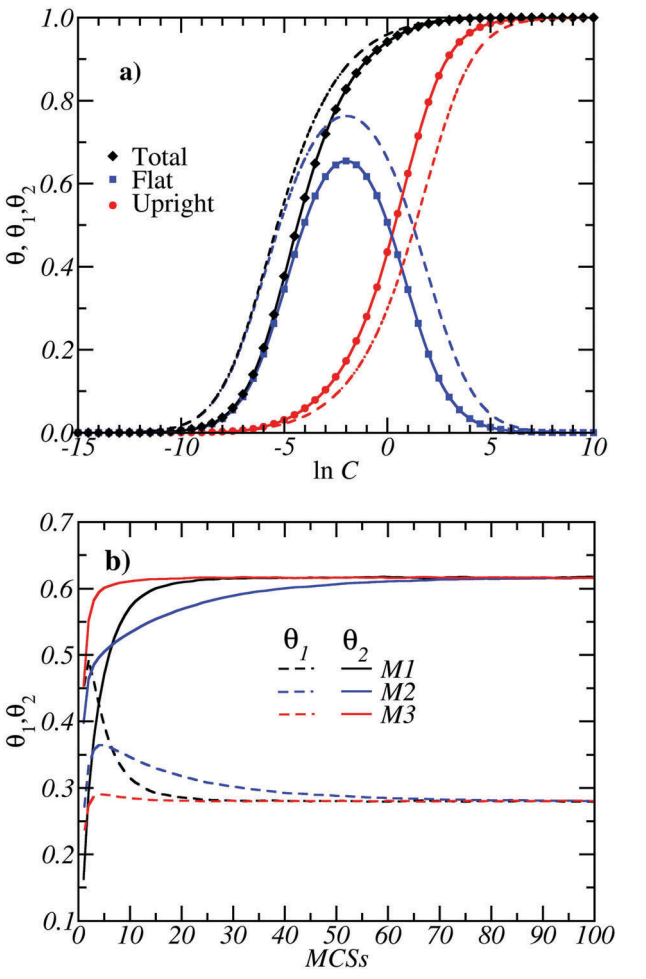

Fig. 2 (a) Total and partial adsorption isotherms (coverage *vs.* $\ln C$) for two-domain AFPs adsorbed on a one-dimensional lattice with $\varepsilon_1/k_BT = -2$ and $\varepsilon_2/k_BT = -4$. Symbols, solid lines and dashed lines represent simulation, LGMMAS [eqn (19)–(21) with $c = 2$] and MLM [eqn (35)–(37)] data, respectively. (b) θ_1 and θ_2 as a function of the number of MCSs for $\ln C = -1$. Black, blue and red lines correspond to results obtained using M1, M2 and M3, respectively.

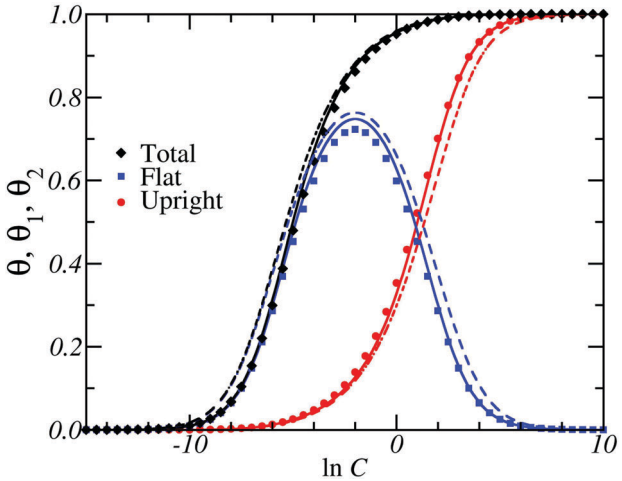

Fig. 3 Total and partial adsorption isotherms for two-domain AFPs adsorbed on a square lattice with $\varepsilon_1/k_BT = -2$ and $\varepsilon_2/k_BT = -4$. Symbols, solid lines and dashed lines represent simulation, LGMMAS [eqn (19)–(21) with $c = 4$] and MLM [eqn (35)–(37)] data, respectively.

In order to understand better this behavior, typical MC configurations corresponding to two-domain proteins adsorbed on a square lattice are shown in Fig. 4. The different panels correspond to different values of the concentration C used. As it can be observed, the proteins adsorb in two alternative conformations: the 1-state or upright configuration (red circles) and the 2-state or flat configuration (blue circles). Green circles represent empty sites. The parameters used in the simulations were: $M = 30 \times 30$, $\varepsilon_1/k_BT = -2$ and $\varepsilon_2/k_BT = -4$.

For low concentration values (top-left panel in Fig. 4), the total adsorption is low, with predominance of proteins adsorbed in the flat orientation. As the concentration increases (top-right and bottom-left panels in Fig. 4), the adsorption of upright proteins starts becoming more favorable and the flat molecules are displaced. Finally, at higher concentrations, the adsorbed phase is constituted almost entirely by upright proteins (bottom-right panel in Fig. 4). This displacement of molecules in the 2-state by molecules in the 1-state is known as the adsorption preference reversal (APR) phenomenon, and has been previously observed in models of competitive adsorption.[30–33]

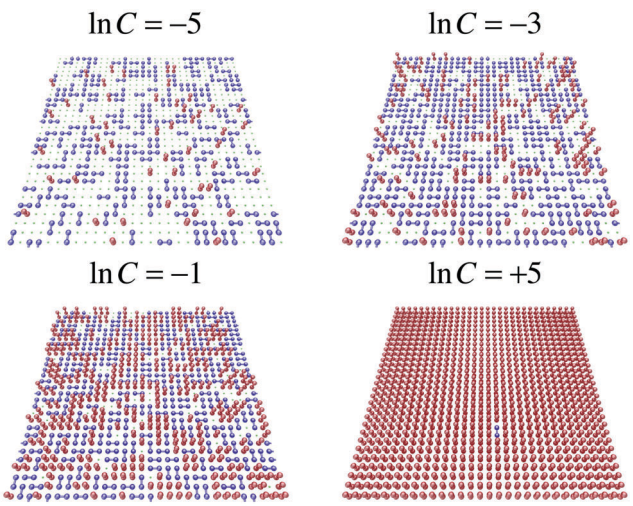

Fig. 4 Typical configurations of the adsorbed phase for different concentrations of the protein in the solution (as indicated). The symbols are as follows: red circle, domain belonging to a protein in the 1-state (upright configuration); blue circle, domain belonging to a protein in the 2-state (flat configuration); and green circle, empty site. In the figure, $M = 30 \times 30$, $\varepsilon_1/k_BT = -2$ and $\varepsilon_2/k_BT = -4$.

With respect to the comparison between theory and simulation, LGMMAS and MLM agree qualitatively well with the MC results. However, LGMMAS leads to appreciably better results than MLM in all ranges of concentrations. Next, and for the sake of simplicity, simulation data will be compared only with LGMMAS predictions.

To complete the analysis of Fig. 3, the adsorption energy per site, configurational entropy per site and Helmholtz free energy per site were calculated as a function of the bulk protein concentration. The results are shown in Fig. 5. Symbols and solid lines represent MC simulation and LGMMAS data, respectively. ε_1/k_BT and ε_2/k_BT are as in previous figures.

The total adsorption energy per site decreases monotonically as C increases, tending asymptotically to $u/k_BT = \varepsilon_1/k_BT$ for higher concentrations. In this limit, the lattice is completely filled by proteins in the 1-state (each molecule with adsorption energy ε_1/k_BT). With respect to the configurational entropy per site, the overall behavior can be summarized as follows. For low concentration values, s/k_B is an increasing function of C, shows a wide maximum at intermediate concentrations, and then decreases monotonically to zero for higher concentrations. In fact, the degeneracy of the structure of the adsorbed phase is equal to one at full coverage, and consequently, $s(\theta \to 1)/k_B = 0$.

The behavior of the Helmholtz free energy per site can be understood by the analysis of the curves of u/k_BT and s/k_B. In all cases, an excellent agreement is observed between theory and MC simulations.

Until this point, the purely additive character of the domain–substrate interaction has been assumed. This is, $\varepsilon_2/k_BT = 2\varepsilon_1/k_BT$,

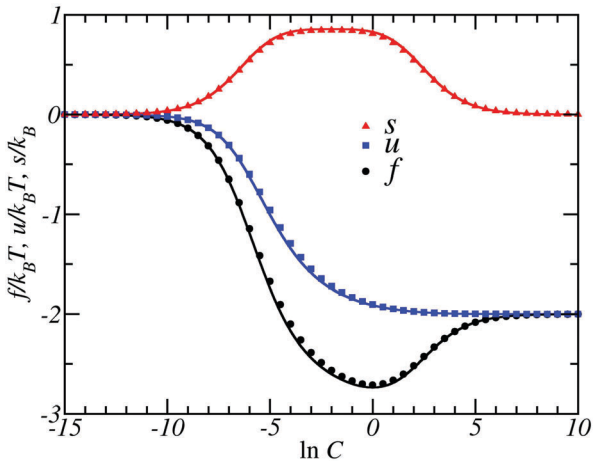

Fig. 5 Adsorption energy per site (in k_BT units), configurational entropy per site (in k_B units) and Helmholtz free energy per site (in k_BT units) for the case studied in Fig. 3. Symbols and solid lines represent simulation and LGMMAS results, respectively.

and the adsorption energy of a molecule in the 2-state (occupying two adsorption sites) is two times the adsorption energy of an isolated domain (occupying one adsorption site). See the values of the parameters in Fig. 2–5.

In more real cases, the adsorption energy of two isolated domains could be different from that corresponding to a molecule in the 2-state. In order to discuss this situation, the simplest model for non-additive domain–substrate interactions will be considered. Namely

$$\varepsilon_2 = 2p\varepsilon_1, \tag{38}$$

where p is the parameter of non-additivity. For $p = 1$, the problem reduces to the additive form. For $p < 1.0$ ($p > 1.0$), each domain–substrate interaction is weaker (stronger) than in the additive case. Then, p emerges as an important control parameter for describing the problem. The implications of such non-additive interactions will be discussed in the following.

Fig. 6 shows the total and partial adsorption isotherms for a square lattice with $\varepsilon_1/k_BT = -2$ and two different values of the parameter of non-additivity p: $p = 0.75$, open symbols; and $p = 1.5$, open symbols. Solid lines denote the theoretical results obtained from LGMMAS, which show a very good agreement with the MC simulation data.

As derived from eqn (38), the larger the value of p, the larger is the absolute value of the adsorption energy of the protein in the 2-state. This situation is reflected in Fig. 6: as the value of p is increased, (1) the adsorption of protein in the flat orientation is favored, (2) the total and flat partial isotherms shift to lower concentrations, and (3) an increase is observed in both the height and width of the curve of θ_2.

In Fig. 7, the effect of the non-additivity parameter on the adsorption energy per site [part (a)] and configurational entropy per site [part (b)] is analyzed. The curves were obtained for $\varepsilon_1/k_BT = -2$ and different values of p: $p = 0.75$, open symbols;

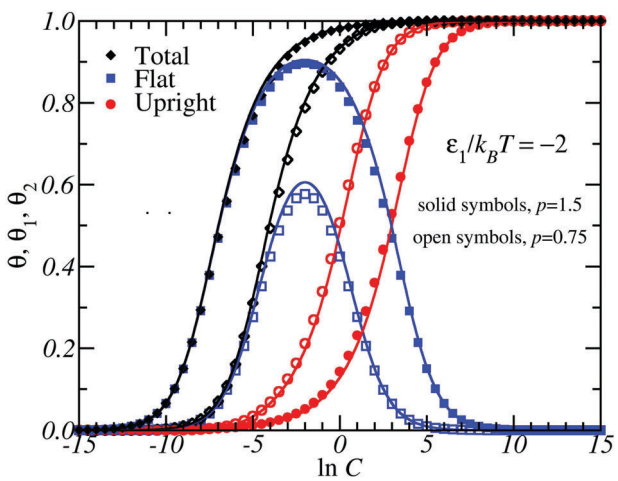

Fig. 6 Total and partial adsorption isotherms for two-domain AFPs adsorbed on a square lattice with $\varepsilon_1/k_BT = -2$, and two different values of the parameter of non-additivity: $p = 0.75$, solid symbols; and $p = 1.5$, open symbols. Symbols and solid lines represent MC simulation and LGMMAS results, respectively.

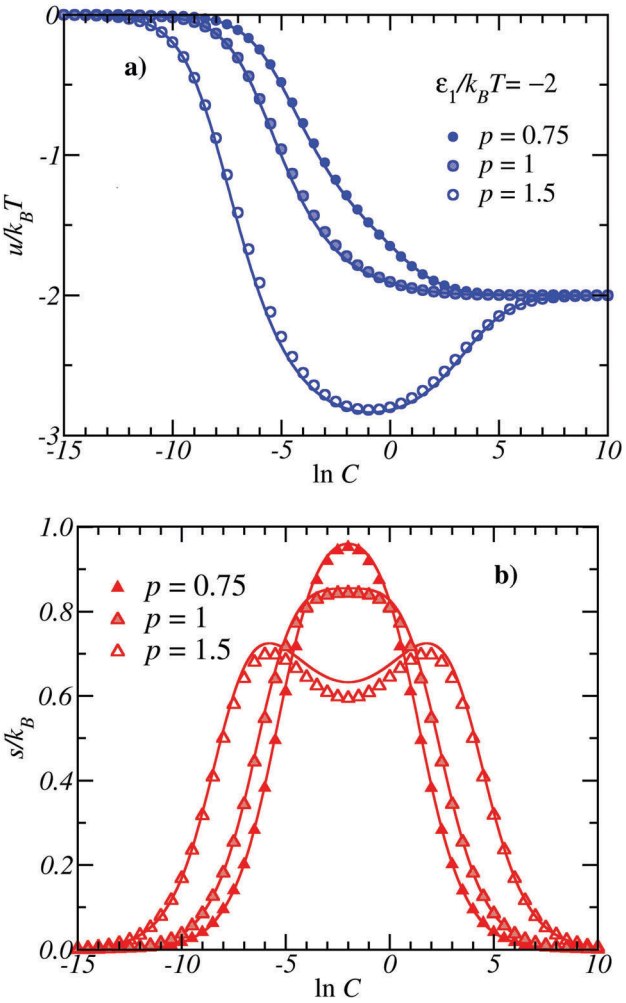

Fig. 7 Adsorption energy per site [part (a)] and configurational entropy per site [part (b)] as a function of the concentration (ln C). The curves were obtained for $\varepsilon_1/k_BT = -2$ and different values of p: $p = 0.75$, open symbols; $p = 1.0$, shaded symbols; and $p = 1.5$, open symbols. Symbols and solid lines represent simulation and LGMMAS results, respectively.

$p = 1.0$, shaded symbols; and $p = 1.5$, open symbols. As in previous figures, an excellent agreement is obtained between theory (lines) and simulation (symbols).

As already reported in Fig. 5 for the additive case ($p = 1.0$), the energy of the adsorbed layer decreases monotonically until the limit value $u/k_BT = \varepsilon_1/k_BT$ is reached. The behavior of u/k_BT is similar for values of $p < 1.0$. However, for $p > 1.0$, a marked minimum is observed in the curve of u/k_BT *vs.* C at an intermediate value of the concentration. In Fig. 7(b), this singularity appears around ln $C \approx -1$. At this value of C, the lattice is almost completely filled by protein molecules adsorbed in flat configurations ($\theta_1 \approx 0.08$ and $\theta_2 \approx 0.88$) [see Fig. 6], and consequently, the energy per site of the adsorbed phase (in k_BT units) is close to $\varepsilon_2/2k_BT$ [-2.7 in Fig. 7(b)]. This value is smaller than the high-concentration energy per site ($\varepsilon_2/2k_BT < \varepsilon_1/k_BT$), and then, a minimum is found in the curve of u/k_BT *vs.* C.

In the case of the entropy per site, Fig. 7(b), an unusual feature is observed for values of the non-additivity parameter

larger than 1. Under these conditions, s/k_B presents a local minimum localized at $\ln C \approx -2$, and two maxima, located at $\ln C \approx -6$ and $\ln C \approx 2$.

The first peak, at $\ln C \approx -6$, occurs when the lattice is occupied by only molecules in the flat orientation (see Fig. 6). This singularity can be easily understood from the dependence on coverage of the configurational entropy per site of dimers adsorbed on a square lattice.[34] As reported in ref. 34, the curve of s/k_B for dimers on square lattices has a maximum for $\theta \approx 0.64$. Then, when the partial isotherm corresponding to flat molecules reaches a value of $\theta_2 \approx 0.64$ [$\ln C \approx -6$, see Fig. 7(a)], the entropy per site shows a first maximum.

The existence of the second peak can be explained following the same arguments given above. In fact, after passing through a maximum near $\ln C \approx -2$, the flat partial isotherm decreases and again takes the value $\theta_2 \approx 0.64$ [$\ln C \approx 2$, see Fig. 7(a)]. At this concentration, $\theta = 1$ (the number of empty sites is equal to zero), and the lattice is completely filled by molecules in the flat orientation and upright proteins. From the point of view of the entropy, the system at $\ln C \approx -6$ (flat proteins and empty sites) has the same number of accessible states as the system at $\ln C \approx 2$ (flat proteins and upright molecules). Accordingly, an identical peak to that observed at $\ln C \approx -6$ appears at $\ln C \approx 2$.

5 Conclusions

In this work, the adsorption of two-domain RD3 antifreeze proteins on ice has been studied by combining theoretical modeling and computational simulations. Two analytical approaches were analyzed: (i) the first (LGMMAS) is based on the exact expression for the partition function of non-interacting linear k-mers adsorbed in one dimension, and its extension to higher dimensions; and (ii) the second (MLM) is a modification of the Langmuir isotherm, which was derived in ref. 16.

In the case of the simulations, a general MC scheme in the grand canonical ensemble was implemented. The ice crystal surface was represented by a square lattice of $M = L \times L$ adsorption sites, and the protein was modeled as a dimer molecule with two possible adsorption states. In addition, following the previous literature, three different adsorption mechanisms were incorporated in the algorithms.

The behavior of the system was characterized by measuring the temperature and coverage dependence of the protein concentration (adsorption isotherm), internal total energy, configurational entropy of the adsorbed phase, and Helmholtz free energy. The results show the adsorption of flat proteins at low concentrations, and a displacement of these molecules by upright proteins at higher concentrations, a phenomenon known as adsorption preference reversal.

For the first time, LGMMAS and MLM were systematically compared with MC simulations. Even though both theoretical formalisms reproduce the main features of the system, LGMMAS appears as the more accurate model in all studied cases. MC results also showed the thermodynamic equivalence of the different adsorption mechanisms proposed in Section 3. This finding has important theoretical implications, demonstrating that the kinetic equations derived in ref. 16 provide equilibrium states directly comparable to the predictions of statistical mechanics models.

It can be concluded that this very simple simulation model (without any special requirement and time consuming computation), combined with a correct theoretical interpretation of the results, can be very useful to obtain a very reasonable description of the adsorption of molecules with multiple conformational states.

Future efforts will be directed to (1) carry out an exhaustive analysis of experimental data, and (2) extend the calculations (theory and simulation) to consider the main kinetic properties of these systems with multiple adsorption states.

A Appendix: acceptance criterion for each MC trial move

The MC method allows us to generate points in configuration space r^N with a relative probability proportional to the Boltzmann factor $\rho(r^N)$ corresponding to the respective ensemble. This is possible for the construction of a Markovian chain that connects directly two consecutive configuration points, Old and New, r^{Old} and r^{New}, respectively. The connection is made by a transition probability from the Old state to the New state, $\Pi(O \rightarrow N)$. This process needs to meet the condition of detailed balance to ensure that the system follows the Boltzmann probability distribution at equilibrium. Then,

$$\rho(r^{Old})\Pi(O \rightarrow N) = \rho(r^{New})\Pi(N \rightarrow O), \quad (39)$$

where $\rho(r^{Old})$ [$\rho(r^{New})$] is the observation probability of the Old [New] state. In addition, the transition probability $\Pi(O \rightarrow N)$ can be written as:

$$\Pi(O \rightarrow N) = \Gamma(O \rightarrow N)\mathrm{acc}(O \rightarrow N), \quad (40)$$

where $\Gamma(O \rightarrow N)$, usually referred to as the underlying matrix of the Markov chain, determines the probability to perform a trial move; and $\mathrm{acc}(O \rightarrow N)$ denotes the probability of accepting or rejecting this trial move. Then, eqn (39) can be rewritten as:

$$\frac{\mathrm{acc}(O \rightarrow N)}{\mathrm{acc}(N \rightarrow O)} = \frac{\rho(r^{New})\Gamma(N \rightarrow O)}{\rho(r^{Old})\Gamma(O \rightarrow N)}. \quad (41)$$

In the original Metropolis scheme, the underlying matrix is chosen to be a symmetric matrix: $\Gamma(O \rightarrow N) = \Gamma(N \rightarrow O)$, which simplified the calculus:

$$\frac{\mathrm{acc}(O \rightarrow N)}{\mathrm{acc}(N \rightarrow O)} = \frac{\rho(r^{New})}{\rho(r^{Old})}. \quad (42)$$

In the present scheme, the underlying matrix is non-symmetrical and the calculation of the acceptance ratio is more complicated than in eqn (42). As an example, let us consider the process of upright adsorption (UA). In this case, the underlying matrix elements can be written as:

$$\Gamma(O \rightarrow N) = P_1/M, \quad \text{(adsorption)} \quad (43)$$

and

Table 2 Acceptance probability ratios and underlying matrix values for each MC trial move. Nomenclature: UA, upright adsorption; FA, flat adsorption; UD, upright desorption; FD, flat desorption; SDA, second domain adsorption; and SDD, second domain desorption

MC trial	$\Gamma(\mathrm{O} \to \mathrm{N})$	$\frac{\mathrm{acc}(\mathrm{O} \to \mathrm{N})}{\mathrm{acc}(\mathrm{N} \to \mathrm{O})}$
UA	$\frac{1}{M}P_1$	$C\exp\left(-\frac{\Delta E}{k_\mathrm{B}T}\right)\frac{P_2}{P_1}$
FA	$\frac{1}{4}\frac{1}{M}(1-P_1)$	$C\exp\left(-\frac{\Delta E}{k_\mathrm{B}T}\right)\frac{1-P_3}{1-P_1}$
UD	$\frac{1}{M}P_2$	$\frac{1}{C}\exp\left(-\frac{\Delta E}{k_\mathrm{B}T}\right)\frac{P_1}{P_2}$
SDA	$\frac{1}{4}\frac{1}{M}(1-P_2)$	$\exp\left(-\frac{\Delta E}{k_\mathrm{B}T}\right)\frac{P_3}{1-P_2}$
SDD	$\frac{1}{4}\frac{1}{M}(1-P_2)$	$\exp\left(-\frac{\Delta E}{k_\mathrm{B}T}\right)\frac{1-P_2}{P_3}$
FD	$\frac{1}{4}\frac{1}{M}(1-P_3)$	$\frac{1}{C}\exp\left(-\frac{\Delta E}{k_\mathrm{B}T}\right)\frac{1-P_1}{1-P_3}$

$$\Gamma(\mathrm{N} \to \mathrm{O}) = P_2/M, \quad \text{(desorption)} \tag{44}$$

where P_1 and P_2 were introduced in Section 3; and the term $1/M$ represents the probability of choosing a site on the lattice (site i, see point 1. in Section 3).

On the other hand, the probabilities $\rho(r^{\mathrm{Old}})$ and $\rho(r^{\mathrm{New}})$ are[22]

$$\rho\left(r^{\mathrm{Old}}\right) \propto \exp\left[\frac{(N-1)\mu - E^{\mathrm{Old}}}{k_\mathrm{B}T}\right], \quad (N-1 \text{ adsorbed particles}) \tag{45}$$

and

$$\rho\left(r^{\mathrm{New}}\right) \propto \exp\left[\frac{N\mu - E^{\mathrm{New}}}{k_\mathrm{B}T}\right], \quad (N \text{ adsorbed particles}) \tag{46}$$

where E^{Old} (E^{New}) is the energy of the Old (New) state, and can be obtained from eqn (1). In addition, μ is the chemical potential.

Introducing eqn (43)–(46) in eqn (41), and by simple algebra, the acceptance ratio corresponding to the case UA results:

$$\frac{\mathrm{acc}(\mathrm{O} \to \mathrm{N})}{\mathrm{acc}(\mathrm{N} \to \mathrm{O})} = C\exp\left(-\frac{\Delta E}{k_\mathrm{B}T}\right)\frac{P_2}{P_1} \tag{47}$$

where $\Delta E = (E^{\mathrm{New}} - E^{\mathrm{Old}})$ is the difference between the energies of the final (New) and initial (Old) states.

The calculations can be easily repeated for all MC trials. The results are shown in Table 2.

Acknowledgements

This work was supported in part by CONICET (Argentina) under project PIP 112-201101-00615; Universidad Nacional de San Luis (Argentina) under project 322000; Universidad Tecnológica Nacional, Facultad Regional San Rafael (Argentina) under project PID UTN 3542 Disp. 284/12 and the National Agency of Scientific and Technological Promotion (Argentina) under project PICT-2013-1678.

References

1 Z. C. Jia and P. L. Davies, *Trends Biochem. Sci.*, 2002, **27**, 101.
2 P. L. Davies, J. Baardsnes, M. J. Kuiper and V. K. Walker, *Philos. Trans. R. Soc. London, Ser. B*, 2002, **357**, 927.
3 Y. Yeh and R. E. Feeney, *Chem. Rev.*, 1996, **96**, 601.
4 K. V. Ewart, Q. Lin and C. L. Hew, *Cell. Mol. Life Sci.*, 1999, **55**, 271.
5 J. A. Raymond and A. L. DeVries, *Proc. Natl. Acad. Sci. U. S. A.*, 1977, **74**, 2589.
6 C. A. Knight, *Nature*, 2000, **406**, 249.
7 C. A. Knight and A. Wierzbicki, Adsorption of Biomolecules to Ice and Their Effects upon Ice Growth. 2. A Discussion of the Basic Mechanism of "Antifreeze" Phenomena, *Cryst. Growth Des.*, 2001, **1**, 439.
8 G. L. Fletcher, C. L. Hew and P. L. Davies, *Annu. Rev. Physiol.*, 2001, **63**, 359.
9 M. H. Kao, G. L. Fletcher, N. C. Wang and C. L. Hew, *Can. J. Zool.*, 1986, **64**, 578.
10 J. H. Wang, *Cryobiology*, 2000, **41**, 1.
11 F. D. Sonnichsen, B. D. Sykes, H. Chao and P. L. Davies, *Science*, 1993, **259**, 1154.
12 C. I. DeLuca, H. Chao, F. D. Sonnichsen, B. D. Sykes and P. L. Davies, *Biophys. J.*, 1996, **71**, 2346.
13 X. Wang, A. L. DeVries and C.-H. C. Cheng, *Biochim. Biophys. Acta, Protein Struct. Mol. Enzymol.*, 1995, **1247**, 163.
14 J. Baardsnes, M. J. Kuiper and P. L. Davies, *J. Biol. Chem.*, 2003, **278**, 38942.
15 N. B. Holland, Y. Nishimiya, S. Tsuda and F. D. Sönnichsen, *Biochemistry*, 2008, **47**, 5935.
16 Ö. Can and N. B. Holland, *J. Colloid Interface Sci.*, 2009, **329**, 24.
17 E. Quiroga and A. J. Ramirez Pastor, *Chem. Phys. Lett.*, 2013, **556**, 330.
18 Ö. Can and N. B. Holland, *Biochemistry*, 2013, **52**, 8745.
19 K. Binder, *Applications of the Monte Carlo Method in Statistical Physics*, Topics in Current Physics, Springer, Berlin, 1984, vol. 36.
20 K. Binder and D. W. Heermann, *Monte Carlo Simulation in Statistical Physics. An Introduction*, Springer, Berlin, 1988.
21 P. Ungerer, B. Tavitian and A. Boutin, *Applications of Molecular Simulation in the Oil and Gas Industry: Monte Carlo Methods*, Editions Technip, Paris, 2005.
22 D. Nicholson and N. G. Parsonage, *Computer Simulation and the Statistical Mechanics of Adsorption*, Academic Press, London, 1982.
23 F. Bulnes, V. Pereyra and J. L. Riccardo, *Phys. Rev. E: Stat. Phys., Plasmas, Fluids, Relat. Interdiscip. Top.*, 1999, **58**, 86.
24 A. Patrykiejew, S. Sokolowski and K. Binder, *Surf. Sci. Rep.*, 2000, **37**, 207.
25 P. Flory, *J. Chem. Phys.*, 1942, **10**, 51.
26 T. Nitta, M. Kuro-Oka and T. Katayama, *J. Chem. Eng. Jpn.*, 1984, **17**, 45; T. Nitta and A. J. Yamaguchi, *J. Chem. Eng. Jpn.*, 1992, **25**, 420.
27 A. J. Ramirez-Pastor, T. P. Eggarter, V. Pereyra and J. L. Riccardo, *Phys. Rev. B: Condens. Matter Mater. Phys.*, 1999, **59**, 11027.

28 T. L. Hill, *An Introduction to Statistical Thermodynamics*, Addison Wesley Publishing Company, Reading, MA, 1960.
29 N. Kubota and J. W. Mullin, *J. Cryst. Growth*, 1995, **152**, 203.
30 K. Ayache, S. E. Jalili, L. J. Dunne, G. Manos and Z. Du, *Chem. Phys. Lett.*, 2002, **362**, 414.
31 L. J. Dunne, G. Manos and Z. Du, *Chem. Phys. Lett.*, 2003, **377**, 551.
32 M. Dávila, J. L. Riccardo and A. J. Ramirez-Pastor, *J. Chem. Phys.*, 2009, **130**, 174715.
33 D. A. Matoz-Fernandez and A. J. Ramirez-Pastor, *Chem. Phys. Lett.*, 2014, **610**, 131.
34 F. Romá, A. J. Ramirez-Pastor and J. L. Riccardo, *Langmuir*, 2000, **16**, 9406.